

The Mass of a Millisecond Pulsar

B. A. Jacoby^{1,2}, A. Hotan^{3,4}, M. Bailes³, S. Ord^{3,5}, and S. R. Kulkarni¹

ABSTRACT

We report on nearly two years of timing observations of the low-mass binary millisecond pulsar, PSR J1909–3744 with the Caltech-Parkes-Swinburne Recorder II (CPSR2), a new instrument that gives unprecedented timing precision. Daily observations give a weighted rms residual of 74 ns, indicating an extremely low level of systematic error. We have greatly improved upon the previous parallax and proper motion measurements of PSR J1909–3744, yielding a distance of $(1.14^{+0.04}_{-0.03})$ kpc and transverse velocity of (200^{+7}_{-6}) km s^{−1}. The system’s orbital eccentricity is just $1.35(12) \times 10^{-7}$, the smallest yet recorded. Since their discovery, the masses of the rapidly rotating millisecond pulsars have remained a mystery, with the recycling hypothesis arguing for heavy objects, and the accretion-induced collapse of a white dwarf more consistent with neutron stars less than the Chandrasekhar limit. Fortuitously, PSR J1909–3744 is an edge-on system, and our data have allowed the measurement of the range and shape of the Shapiro delay to high accuracy, giving the first precise determination of a millisecond pulsar mass to date, $m_p = (1.438 \pm 0.024) M_\odot$. The mass of PSR J1909–3744 is at the upper edge of the range observed in mildly recycled pulsars in double neutron star systems, consistent with the recycling hypothesis. It appears that the production of millisecond pulsars is possible with the accretion of less than $0.2 M_\odot$.

Subject headings: binaries:close — pulsars: individual(PSR J1909–3744) — relativity — stars: distances — stars: fundamental parameters — stars: neutron

¹Department of Astronomy, California Institute of Technology, MS 105-24, Pasadena, CA 91125; srk@astro.caltech.edu.

²present address: Naval Research Laboratory, Code 7213, 4555 Overlook Avenue, SW, Washington, DC 20375; bryan.jacoby@nrl.navy.mil.

³Centre for Astrophysics and Supercomputing, Swinburne University of Technology, P.O. Box 218, Hawthorn, VIC 31122, Australia; ahotan@astro.swin.edu.au, mbales@astro.swin.edu.au.

⁴Australia Telescope National Facility, CSIRO, P.O. Box 76, Epping, NSW 1710, Australia.

⁵present address: School of Physics, University of Sydney, A28, NSW 2006, Australia; ord@physics.usyd.edu.au.

1. Introduction

Radio pulsars in binary systems can allow the measurement of neutron star masses, thereby providing one side of the dense matter equation of state. However, to date all pulsars with precisely-measured masses have been relatively slowly rotating objects (spin period P typically tens of milliseconds) in double neutron star systems or, in one case, an eccentric pulsar-massive white dwarf system (see Stairs, 2004 for a recent review). These neutron stars all fall within the narrow mass range of $(1.35 \pm 0.04) M_{\odot}$ established by Thorsett & Chakrabarty (1999), with the exception of PSR B1913+16 at $(1.4408 \pm 0.0003) M_{\odot}$ (Weisberg & Taylor 2003) and PSR J0737–3039B at $(1.250 \pm 0.005) M_{\odot}$ (Lyne et al. 2004).

Millisecond pulsars ($P < 10$ ms) are generally thought to have accreted more matter from a low-mass binary companion and therefore are expected to be more massive than the slower-rotating recycled pulsars with massive companions. However, these low-mass binary pulsars do not experience measurable relativistic orbital period decay (\dot{P}_b) and their typically circular orbits make orbital precession ($\dot{\omega}$) and time dilation and gravitational redshift (γ) difficult to measure; therefore, mass determinations have been less precise. There is a statistical suggestion that millisecond pulsars are indeed more massive than slower-rotating neutron stars (Kaspi et al. 1994; van Straten et al. 2001; Freire et al. 2003), but with the exception of PSR J0751+1807 at $(2.1 \pm 0.2) M_{\odot}$ (Nice et al., in preparation; Nice et al. 2004) and possibly PSR J1748-2446I in the globular cluster Terzan 5 (Ransom et al. 2005), all are still consistent with the observed mass distribution of pulsars with massive companions.

PSR J1909–3744 was discovered during a large-area survey for pulsars at high galactic latitudes with the 64-m Parkes radio telescope (Jacoby et al. 2003). It is a typical low-mass binary pulsar with $P = 2.95$ ms, but with several exceptional qualities: its extremely narrow pulse profile (Ord et al. 2004) and stable rotation allow us to measure pulse arrival times with unprecedented precision, and its nearly edge-on orbital inclination means the pulsar signal experiences strong Shapiro delay. Measurement of this Shapiro delay gives the orbital inclination and companion mass to high precision, and when combined with the Keplerian orbital parameters, allows us to measure the pulsar’s mass.

2. Observations and Pulse Timing

In December 2002, we began observing PSR J1909–3744 with the Caltech-Parkes-Swinburne Recorder II (CPSR2, see Bailes 2003) at the Parkes radio telescope. This instrument samples the voltage signal from the telescope in each of two 64-MHz wide dual-

polarization bands with 2-bit precision. For these observations, we used the center beam of the Parkes Multibeam receiver or H-OH receiver and placed the two bands at sky frequencies of 1341 MHz and 1405 MHz. The raw voltage data were sent to a dedicated cluster of 30 dual-processor Xeon computers for immediate analysis. The two-bit sampled data were corrected for quantization effects (Jenet & Anderson 1998) and coherently dedispersed into 128 frequency channels in each of 4 Stokes parameters which were then folded at the topocentric pulse period using the PSRDISP software package (van Straten 2002). We recently began observing PSR J1909–3744 with the Caltech-Green Bank-Swinburne Recorder II (CGSR2), a clone of CPSR2 installed at the 100-m Green Bank Telescope (GBT). As our current GBT data set covers only a small fraction of the system’s orbital phase, we have not included it in this analysis.

Off-line data reduction and calculation of average pulse times of arrival (TOAs) were accomplished in the usual manner using the PSRCHIVE¹ suite. Because of roll-off of the anti-aliasing filters, 8 MHz was removed from each band edge prior to formation of dedispersed total intensity profiles, giving a final bandwidth of 48 MHz per band. To avoid averaging over phenomena which vary on orbital timescales, observations longer than 10 minutes were broken into 10-minute segments. Finally, TOAs were calculated by cross-correlation with a high signal-to-noise template profile, formed by summing a total of 5.4 days of integration in the 1341 MHz band. Arrival times with uncertainty greater than $1\,\mu\text{s}$ were excluded from further analysis. Our final data set contains 1730 TOAs – roughly half of which come from each of our two frequency bands.

We used the standard pulsar timing package TEMPO², along with the Jet Propulsion Laboratory’s DE405 ephemeris, for all timing analysis. TOAs were corrected to UTC(NIST). Using the TOA uncertainties estimated from the cross-correlation procedure, our best-fit timing model had reduced $\chi^2 \simeq 1.2$, indicating that our arrival time measurements are relatively free of systematic errors. In our final analysis, these TOA uncertainties were scaled by a factor of 1.1 to achieve a reduced $\chi^2 \simeq 1$ and improve our estimation of uncertainties in model parameters. Because TEMPO estimates parameter uncertainties based on the assumption that the reduced χ^2 is unity, and because TOA uncertainties normally must be scaled by significantly larger factors to satisfy this assumption, it has become customary to take twice the formal error from TEMPO as the $1\,\sigma$ uncertainty to compensate for systematic errors. We have not followed this practice as our scaling factor is nearly unity. Because of the system’s low eccentricity (e), we used the ELL1 binary model which replaces the longi-

¹<http://astronomy.swin.edu.au/pulsar/software/libraries/>

²<http://pulsar.princeton.edu/tempo/>

tude of periastron (ω), time of periastron (T_0), and e with the time of ascending node (T_{asc}) and the Laplace-Lagrange parameters $e \sin \omega$ and $e \cos \omega$ (Lange et al. 2001). The resulting parameter values are all consistent with those obtained using the DD model (Damour & Deruelle 1985, 1986), though the estimated uncertainties of several orbital parameters differ significantly. We give the results of our timing analysis in Table 1. Although the rms timing residual could be lowered to 74 ns by integrating our daily observations, high time resolution around superior conjunction was vital in mapping the Shapiro delay of the pulsar. The weighted rms residual of only 230 ns obtained from 10-minute integrations in each of the two bands is still exceptional.

2.1. Shapiro Delay and Component Masses

As shown in Figure 1, our timing data display the unmistakable signature of Shapiro delay. Measurement of this relativistic effect has allowed the precise determination of orbital inclination, $i = (86.58^{+0.11}_{-0.10})^\circ$, and companion mass, $m_c = (0.2038 \pm 0.0022) M_\odot$. These values were derived from a χ^2 map in $m_c - \cos i$ space (Fig. 2), but are in excellent agreement with the results of TEMPO’s linear least-squares fit for m_c and $\sin i$.

Combined with the mass function, our tight constraints on m_c and i determine the pulsar mass, $m_p = (1.438 \pm 0.024) M_\odot$ (Fig. 3). This result is several times more precise than the previous best mass measurements of heavily recycled neutron stars.

We have used Shapiro delay to measure two post-Keplerian parameters for this system, shape $s \equiv \sin i = 0.99822 \pm 0.00011$ and range $r \equiv m_c G/c^3 = (1.004 \pm 0.011) \mu\text{s}$, where G is the gravitational constant and c is the speed of light. The value of $\dot{\omega}$ predicted by general relativity is only 0.14 deg yr^{-1} , so it will be many years before a third post-Keplerian parameter can be measured in this extremely circular system. We note that PSR J1909–3744 has the smallest eccentricity of any known system, $e = 1.35(12) \times 10^{-7}$.

2.2. Distance and Kinematic Effects

The measured parallax, $\pi = (0.88 \pm 0.03) \text{ mas}$ gives a distance of $d_\pi = (1.14^{+0.04}_{-0.03}) \text{ kpc}$. We can now calculate the mean free electron density along the line of sight to PSR J1909–3744 based on its dispersion measure (DM), $\langle n_e \rangle \equiv DM/d = DM\pi = (0.0091 \pm 0.0003) \text{ cm}^{-3}$. The DM -derived distance estimate is 0.46 kpc (Cordes & Lazio 2002), indicating that the free electron density along the line of sight is significantly overestimated by the model. There are no pulsars near PSR J1909–3744 on the sky with accurate parallax measurements, either

through pulse timing or interferometry; PSR J1909–3744 will therefore provide an important constraint on galactic electron density models.

The pulsar’s proper motion induces an apparent secular acceleration equal to $\mu^2 d/c$ (Shklovskii 1970). The secular acceleration corrupts the observed period derivative (\dot{P}). Since the pulsar’s intrinsic spindown rate must be non-negative, we can obtain an upper distance limit of $d_{\text{max}} = 1.4 \text{ kpc}$, consistent with the measured parallax. Conversely, the measured proper motion and parallax-derived distance allow us to correct for the secular acceleration and determine the intrinsic spindown rate, \dot{P}_{int} , which we then use to calculate the characteristic age, $\tau_c = P/(2\dot{P}_{\text{int}})$, and surface dipole magnetic field, $B_{\text{surf}} = 3.2 \times 10^{19} (P\dot{P}_{\text{int}})^{1/2} \text{ G}$ (Tab. 1). We note that the acceleration induced by differential Galactic rotation is about two orders of magnitude smaller than the secular acceleration and has therefore been neglected.

Similarly, the secular acceleration induces an apparent \dot{P}_b . Based on the distance and proper motion of PSR J1909–3744, this kinematic \dot{P}_b is expected to be $\sim 0.5 \times 10^{-12}$ – about 400 times larger (and of opposite sign) than the predicted intrinsic value. We note that if we include \dot{P}_b in our timing model, the best-fit value is consistent with this prediction but the significance is low. Therefore, we have not included \dot{P}_b in our analysis. However, in several years, this kinematic \dot{P}_b will give an improved measurement of the pulsar distance (Bell & Bailes 1996).

The transverse velocity resulting from the parallax distance and the measured proper motion is $(200^{+7}_{-6}) \text{ km s}^{-1}$, somewhat higher than typical for binary millisecond pulsars (Toscano et al. 1999). We note that, in the absence of the parallax distance measurement, we would have significantly underestimated the system’s velocity.

3. Conclusions

We have obtained the most precise mass of a heavily recycled neutron star through high-precision timing measurements of PSR J1909–3744: $m_p = (1.438 \pm 0.024) M_{\odot}$. While PSR J1909–3744 appears to be more massive than the canonical range for mildly recycled pulsars ($1.35 \pm 0.04 M_{\odot}$), its mass is consistent with that of the original member of this class, namely PSR B1913+16. Therefore, it is unlikely that a clear mass distinction can be made between the millisecond pulsars with low-mass white dwarf companions and the mildly recycled pulsars with massive companions.

It is possible that neutron star birth masses are simply not as homogeneous as the sample of measurements suggested until recently. The discovery of PSR J0737–3039B in

the double pulsar system with $m_p = (1.250 \pm 0.005) M_\odot$ is difficult to reconcile with the millisecond pulsars PSR J0751+1807 and PSR J1748-2446I, with most probable masses near or exceeding $2 M_\odot$, based purely on post-supernova accretion history. If we assume that the mass of PSR J0737–3039B (the only well-measured slow pulsar mass and the lowest measured neutron star mass) is representative of pre-accretion neutron stars, it appears that the accretion of less than $0.2 M_\odot$ is sufficient for spinning pulsars up to millisecond periods, implying that most of the companion’s original mass may be lost from the system. On the other hand, the more massive MSPs suggest that, in some cases, the accreted mass is several times larger.

Shortly after their discovery, it was proposed that millisecond pulsars were produced from normal neutron stars that were recycled by the accretion of matter (Alpar et al. 1982). However an alternative hypothesis was put forward by Bailyn & Grindlay (1990) in which millisecond pulsars were created by the accretion induced collapse of a white dwarf. In this scenario, the millisecond pulsar should be less than the Chandrasekhar mass minus the binding energy that is realized upon collapse of the neutron star. PSR J1909–3744’s mass suggests that the recycling process is more probable.

The timing precision of PSR J1909–3744 with a 64-m class telescope is extraordinary. Every 10 minutes, CPSR2 yields two arrival times with a weighted rms residual of just 230 ns. By integrating the data further, we found we could reduce the residual to just 74 ns, but there is reason to believe that we can reduce this figure still further. At present typical integrations are only an hour, and there is potentially 512 MHz of bandwidth at 20 cm available for precision timing at the Parkes telescope, only 128 MHz of which is used by the CPSR2 instrument. Longer observations with four times the bandwidth could potentially yield arrival times with an integrated rms residual of just a few tens of ns. Such precision would allow us to probe the Universe for the signature of supermassive black hole binaries because of the effect of gravitational waves on timing measurements (Jaffe & Backer 2003; Lomen et al. 2003).

We acknowledge S. Anderson, W. van Straten, J. Yamasaki, and J. Maciejewski for major contributions to the development of CPSR2, and thank H. Knight for assistance with observations. These data contain some arrival times from the P456 program of R. Manchester et al. BAJ and SRK thank NSF and NASA for supporting their research. The Parkes telescope is part of the Australia Telescope which is funded by the Commonwealth of Australia for operation as a National Facility managed by CSIRO.

REFERENCES

- Alpar, M. A., Cheng, A. F., Ruderman, M. A., & Shaham, J. 1982, *Nature*, 300, 728
- Bailes, M. 2003, in *ASP Conference Series*, Vol. 302, *Radio Pulsars*, ed. M. Bailes, D. J. Nice, & S. E. Thorsett (Astronomical Society of the Pacific), 57–64
- Bailyn, C. D. & Grindlay, J. E. 1990, *ApJ*, 353, 159
- Bell, J. F. & Bailes, M. 1996, *ApJ*, 456, L33
- Cordes, J. M. & Lazio, T. J. W. 2002, *astro-ph/0207156*
- Damour, T. & Deruelle, N. 1985, *Ann. Inst. H. Poincaré (Physique Théorique)*, 43, 107
- . 1986, *Ann. Inst. H. Poincaré (Physique Théorique)*, 44, 263
- Freire, P. C., Camilo, F., Kramer, M., Lorimer, D. R., Lyne, A. G., Manchester, R. N., & D’Amico, N. 2003, *MNRAS*, 340, 1359
- Jacoby, B. A., Bailes, M., van Kerkwijk, M. H., Ord, S., Hotan, A., Kulkarni, S. R., & Anderson, S. B. 2003, *ApJ*, 599, L99
- Jaffe, A. H. & Backer, D. C. 2003, *ApJ*, 583, 616
- Jenet, F. A. & Anderson, S. B. 1998, *PASP*, 110, 1467
- Kaspi, V. M., Taylor, J. H., & Ryba, M. 1994, *ApJ*, 428, 713
- Lange, C., Camilo, F., Wex, N., Kramer, M., Backer, D., Lyne, A., & Doroshenko, O. 2001, *MNRAS*, 326, 274
- Lomen, A. N., Backer, D. C., & Nice, E. M. S. D. J. 2003, in *ASP Conference Series*, Vol. 302, *Radio Pulsars*, ed. M. Bailes, D. J. Nice, & S. E. Thorsett (Astronomical Society of the Pacific), 81–84
- Lyne, A. G., Burgay, M., Kramer, M., Possenti, A., Manchester, R. N., Camilo, F., McLaughlin, M. A., Lorimer, D. R., D’Amico, N., Joshi, B. C., Reynolds, J., & Freire, P. C. C. 2004, *Science*, 303, 1153
- Nice, D. J., Splaver, E. M., & Stairs, I. H. 2004, *astro-ph/0411207*
- Ord, S. M., van Straten, W., Hotan, A. W., & Bailes, M. 2004, *MNRAS*, 352, 804

- Ransom, S. M., Hessels, J. W. R., Stairs, I. H., Freire, P. C. C., Camilo, F., Kaspi, V. M., & Kaplan, D. L. 2005, *Science*, 307, 892
- Shklovskii, I. S. 1970, *Sov. Astron.*, 13, 562
- Stairs, I. H. 2004, *Science*, 304, 547
- Thorsett, S. E. & Chakrabarty, D. 1999, *ApJ*, 512, 288
- Toscano, M., Sandhu, J. S., Bailes, M., Manchester, R. N., Britton, M. C., Kulkarni, S. R., Anderson, S. B., & Stappers, B. W. 1999, *MNRAS*, 307, 925
- van Straten, W. 2002, *ApJ*, 568, 436
- van Straten, W., Bailes, M., Britton, M., Kulkarni, S. R., Anderson, S. B., Manchester, R. N., & Sarkissian, J. 2001, *Nature*, 412, 158
- Weisberg, J. M. & Taylor, J. H. 2003, in *ASP Conference Series*, Vol. 302, *Radio Pulsars*, ed. M. Bailes, D. J. Nice, & S. E. Thorsett (Astronomical Society of the Pacific), 93–98

Table 1. Improved parameters of the PSR J1909–3744 system

Parameter	Value ^a
Right ascension, α_{J2000}	19 ^h 09 ^m 47 ^s .4379988(6)
Declination, δ_{J2000}	−37°44′14″.31841(4)
Proper motion in α , μ_α (mas yr ^{−1})	−9.470(11)
Proper motion in δ , μ_δ (mas yr ^{−1})	−35.76(8)
Annual parallax, π (mas)	0.88(3)
Pulse period, P (ms)	2.947108021647488(3)
Period derivative, \dot{P} (10 ^{−20})	1.40258(4)
Reference epoch (MJD)	53000.0
Dispersion measure, DM (pc cm ^{−3})	10.39392(6)
Binary period, P_b (d)	1.533449450441(10)
Projected semimajor axis, $a \sin i$ (lt-s) ..	1.89799117(4)
$e \sin \omega$ ($\times 10^{-7}$)	0.56(18)
$e \cos \omega$ ($\times 10^{-7}$)	−1.24(10)
Time of ascending node, T_{asc} (MJD)	53000.4753280898(13)
$\sin i$	0.99822(11)
Companion mass m_c (M_\odot)	0.2038(22)
Derived Parameters	
Pulsar mass m_p (M_\odot)	1.438(24)
Mass function, $f(m)$	0.0031219531(2)
Range of Shapiro delay, r (μs)	1.004(11)
Orbital inclination, i (deg)	86.58 ^{+0.11} _{−0.10}
Orbital eccentricity, e ($\times 10^{-7}$)	1.35(12)
Longitude of periastron, ω (deg)	155.7452858095 \pm 7
Time of periastron, T_0	53001.13873788 \pm 0.03
Parallax distance, d_π (kpc)	1.14 ^{+0.04} _{−0.03}
Transverse velocity, v_\perp (km s ^{−1})	200 ⁺⁷ _{−6}
Intrinsic period derivative, \dot{P}_{int} (10 ^{−20}) ^b	0.28(4)
Surface magnetic field, B_{surf} ($\times 10^8$ G) ^b ..	0.92 ^{+0.06} _{−0.07}
Characteristic age, τ_c (Gyr) ^b	16 ⁺³ _{−2}
Galactic longitude, l (deg)	359.73
Galactic latitude, b (deg)	−19.60
Distance from Galactic plane, $ z $ (kpc) ..	0.383(12)

^aFigures in parenthesis are uncertainties in the last digit quoted. The formal error calculated by TEMPO is taken as the 1 σ uncertainty, except as described in §2.1; all quoted uncertainties correspond to the 68.3% confidence interval.

^bCorrected for secular acceleration based on measured proper motion and parallax

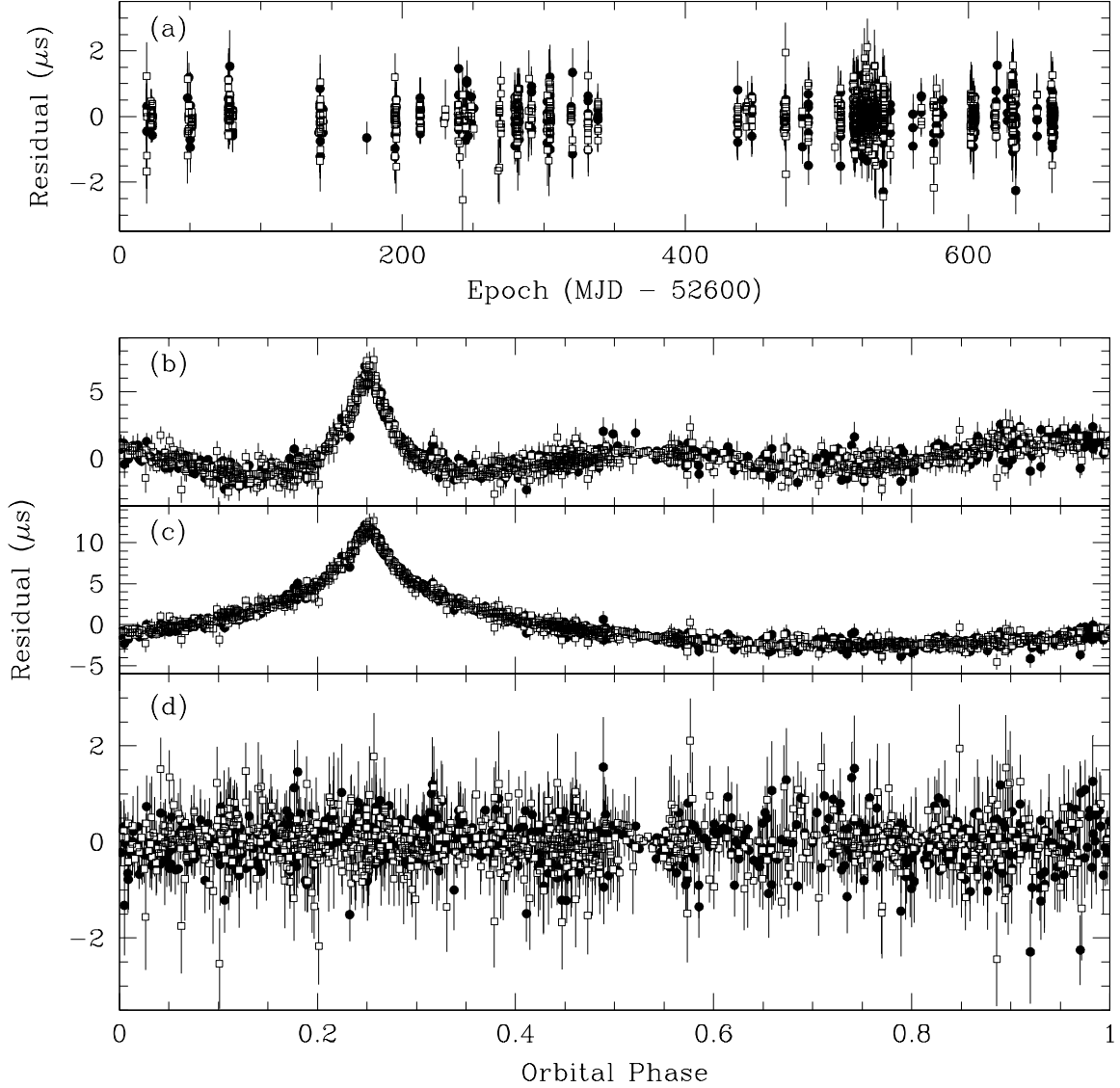


Fig. 1.— High-precision timing residuals for PSR J1909–3744. Filled circles represent TOAs from 1341 MHz band, while open squares denote the 1405 MHz band. (a): Residuals vs. observation epoch for best-fit model taking Shapiro delay fully into account (Tab. 1). (b): Residuals vs. orbital phase for best-fit Keplerian model. Some of the Shapiro delay signal is absorbed in an anomalously large Roemer delay and eccentricity. (c): Residuals vs. orbital phase for the best-fit model, but with the companion mass set to zero (i.e. the correct Keplerian orbit, but neglecting Shapiro delay). (d): Residuals vs. orbital phase for the best-fit model taking Shapiro delay fully into account (Tab. 1).

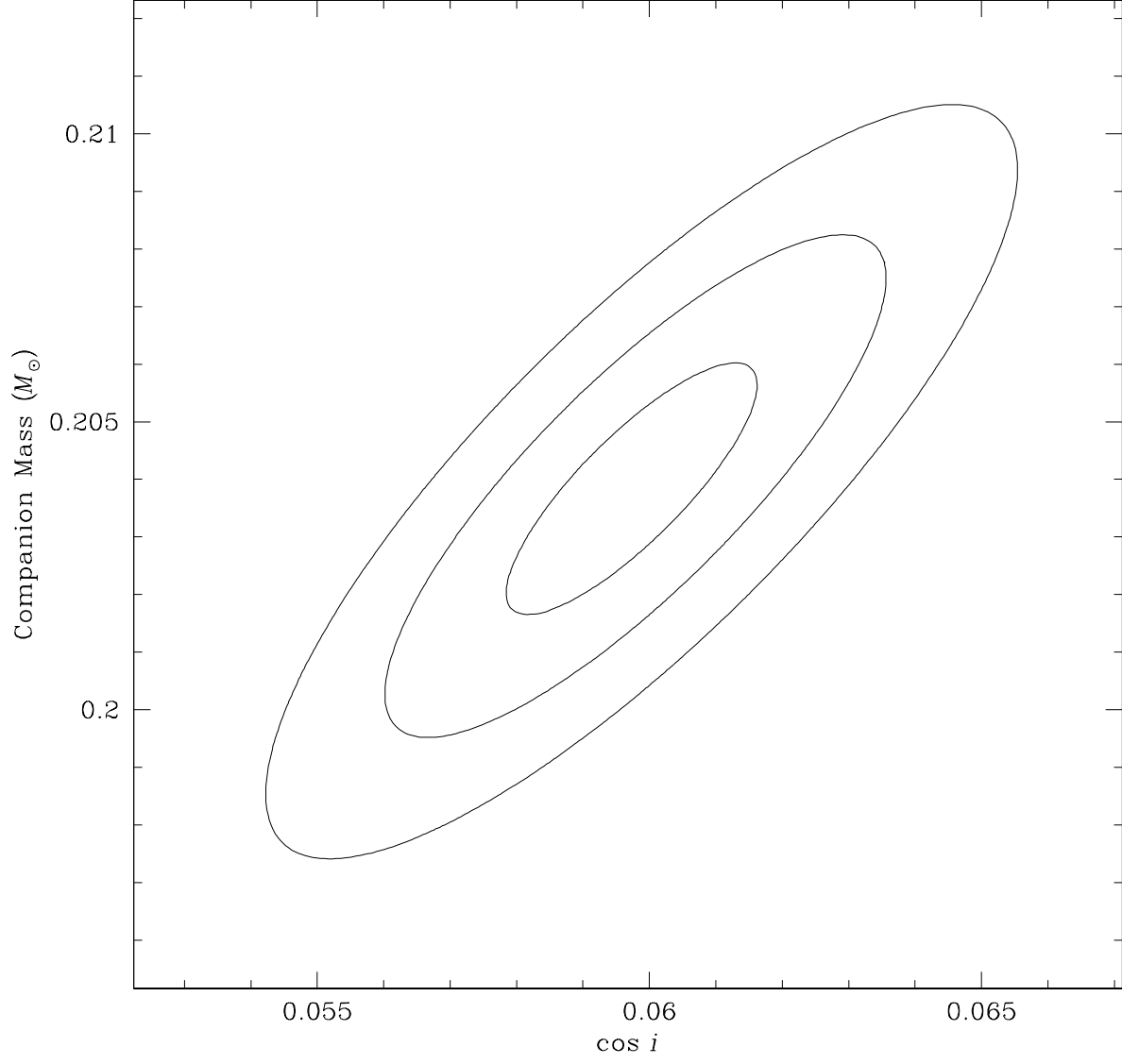


Fig. 2.— Companion mass – orbital inclination diagram for PSR J1909–3744. Contours show $\Delta\chi^2 = 1, 4$, and 9 ($1\sigma, 2\sigma$, and 3σ , or 68.3%, 95.4%, and 99.7% confidence) regions, respectively in companion mass and $\cos i$.

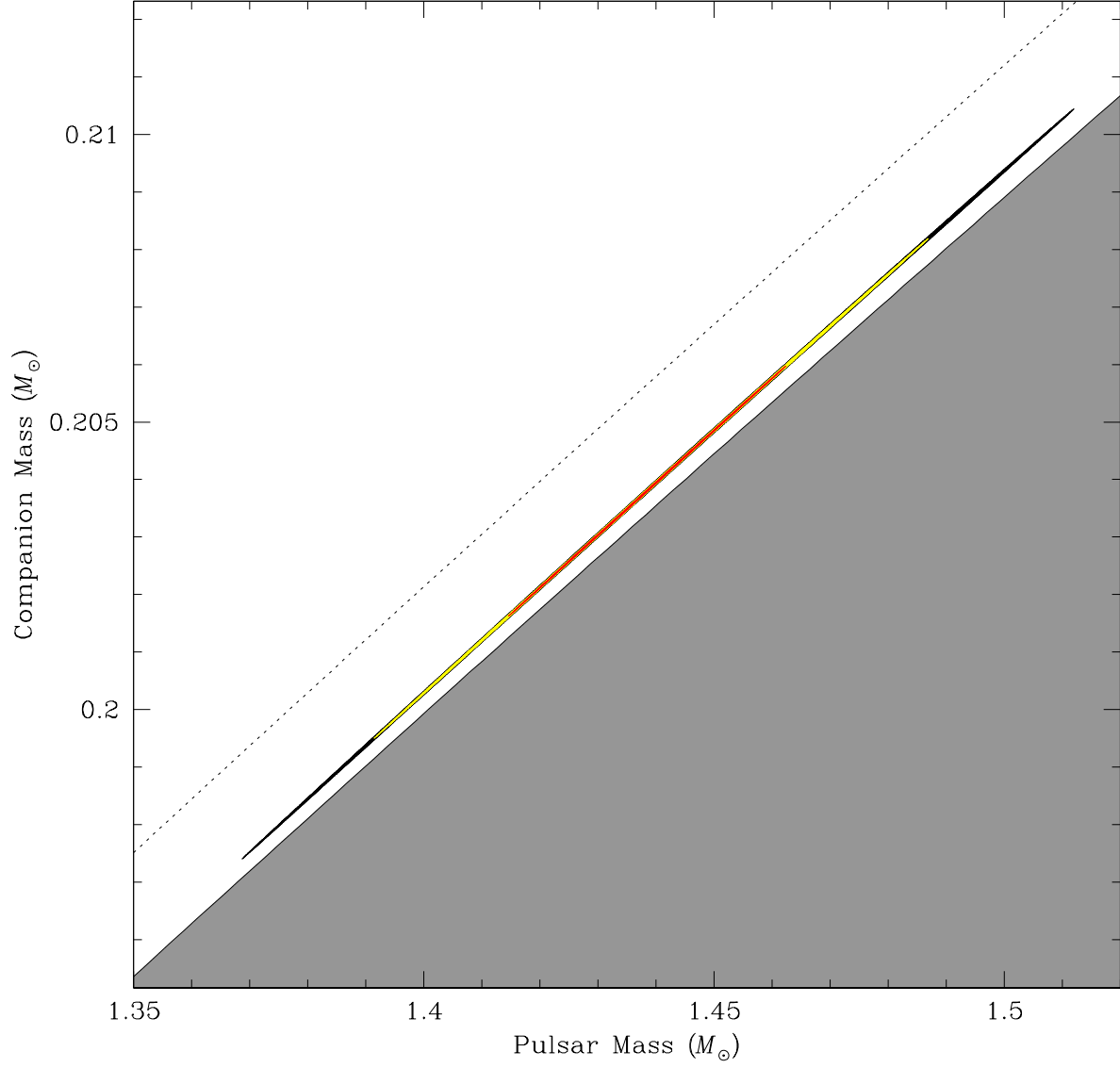


Fig. 3.— Mass-mass diagram for PSR J1909–3744. Red, yellow, and black areas show $\Delta\chi^2 = 1$, 4, and 9 (1σ , 2σ , and 3σ , or 68.3%, 95.4%, and 99.7% confidence) regions, respectively in companion mass and pulsar mass. The grey shaded region is excluded by the mass function and the requirement that $\sin i \leq 1$; the dotted line indicates $\sin i = 0.99$ for reference.